09.3

Investigation of amplified radiation wavefront distortions in a cryogenically cooled laser amplifier

© V.A. Petrov[1,2], V.V. Petrov[1–3], G.V. Kuptsov[1,2], A.O. Kuptsova[1,3]

[1] Institute of Laser Physics of the Siberian Branch of the Russian Academy of Sciences, Novosibirsk, Russia
[2] Novosibirsk State Technical University, Novosibirsk, Russia
[3] Novosibirsk State University, Novosibirsk, Russia
E-mail: petrov.nstu@gmail.com

Received May 17, 2024
Revised June 27, 2024
Accepted June 28, 2024

Thermal and electronic contributions to wavefront distortions of radiation amplified in the cryogenically cooled amplifier have been investigated using the laser scanning technique. The optical path difference profile introduced for amplified radiation with the pulse repetition rate of 200–1000 Hz and pump radiation peak power of 200 W have been analyzed.

Keywords: diode pumping, high pulse repetition rate, cryogenic temperatures, wavefront distortions.

DOI: 10.61011/TPL.2024.10.59704.19996

One of the trends in experimental laser physics development is creation of laser systems generating pulses with high peak and average powers. Such systems find various applications, including studying nonlinear interaction of intense radiation with matter [1,2]. Multichannel and multistage laser amplifiers, e.g. those with active elements of complex configuration [3–5], are used in laser setups to obtain high radiation intensities. This gives rise to a wide class of problems in ensuring stability, high quality, and controllability of the amplified radiation parameters.

This paper is devoted to studying the mechanisms of amplified pulse wavefront distortions associated with the process of laser amplification. Differences between optical paths of waves passing through different active element regions arise due to variations in the refractive index. The optical path difference between the wave passing through the pumped region center and other waves consists of component $\Delta\varphi_T$ associated with temperature and component $\Delta\varphi_N$ associated with the medium polarizability [6–8]:

$$\Delta\varphi_T(x,y) = \left[\frac{dn\big(T(x,y)\big)}{dT} + 2n_0^3 C\alpha_T\big(T(x,y)\big) + (n_0-1)(1+\nu)\alpha_T\big(T(x,y)\big)\right]\langle T(x,y)-T_0\rangle L,$$

$$\Delta\varphi_N(x,y) = \frac{2\pi}{n_0}\left(\frac{n_0^2+2}{3}\right)^2 pN(x,y)L, \qquad (1)$$

where x and y are the coordinates in the plane perpendicular to the radiation propagation direction [mm], dn/dT is the temperature dependence of the medium refractive index variation [K^{-1}], n_0 is the medium refractive index, C is the photoelasticity coefficient, α_T is the thermal expansion coefficient [K^{-1}], ν is the Poisson's ratio, $\langle T(x,y)-T_0\rangle$ is the difference between the active element temperature at the point with coordinates x, y and temperature in the pump spot center averaged along the direction of radiation propagation [K], L is the medium length [cm], p is the difference between active ion polarizabilities in the excited and nonexcited states [cm^3], N is the upper level population [cm^{-3}].

Requirements for time resolution of the device used to study the dynamics of wavefront distortions are based on characteristic times of the thermal and electronic components of the refractive index variations. Commercially available wavefront detectors (Shack–Hartmann sensors) are based on CCD matrices, which limits their response rate. One of the ways to solve the problem of response rate is to calculate the optical path difference (OPD) from the experimentally measured temperature field and upper level population in the active element. The method is based on the temperature dependence of the Yb^{3+} ions absorption crosssection at the amplification wavelength of 1030 nm [9]. The method's response rate is caused by the use of photodiodetectors. The upper level population will be determined based on experimentally measured gain G:

$$N = \frac{\ln G/L + f_L(T)\sigma(T)N_t}{\sigma(T)\cdot\big(f_L(T)+f_U(T)\big)}, \qquad (2)$$

where $\sigma(T)$ is the gain crosssection [cm^2], $f_L(T)$ and $f_U(T)$ are the ground and working level populations according to the Boltzmann statistics, N_t is the concentration of activator ions [cm^{-3}].

Formula (2) shows that the temperature distribution should be taken into account in determining both the thermal and electronic components of the refractive index variation. Therewith, the measured gain value does not affect determination of the thermal component. The thermal component depends on the procedures of medium heating and cooling with durations of the order of seconds.

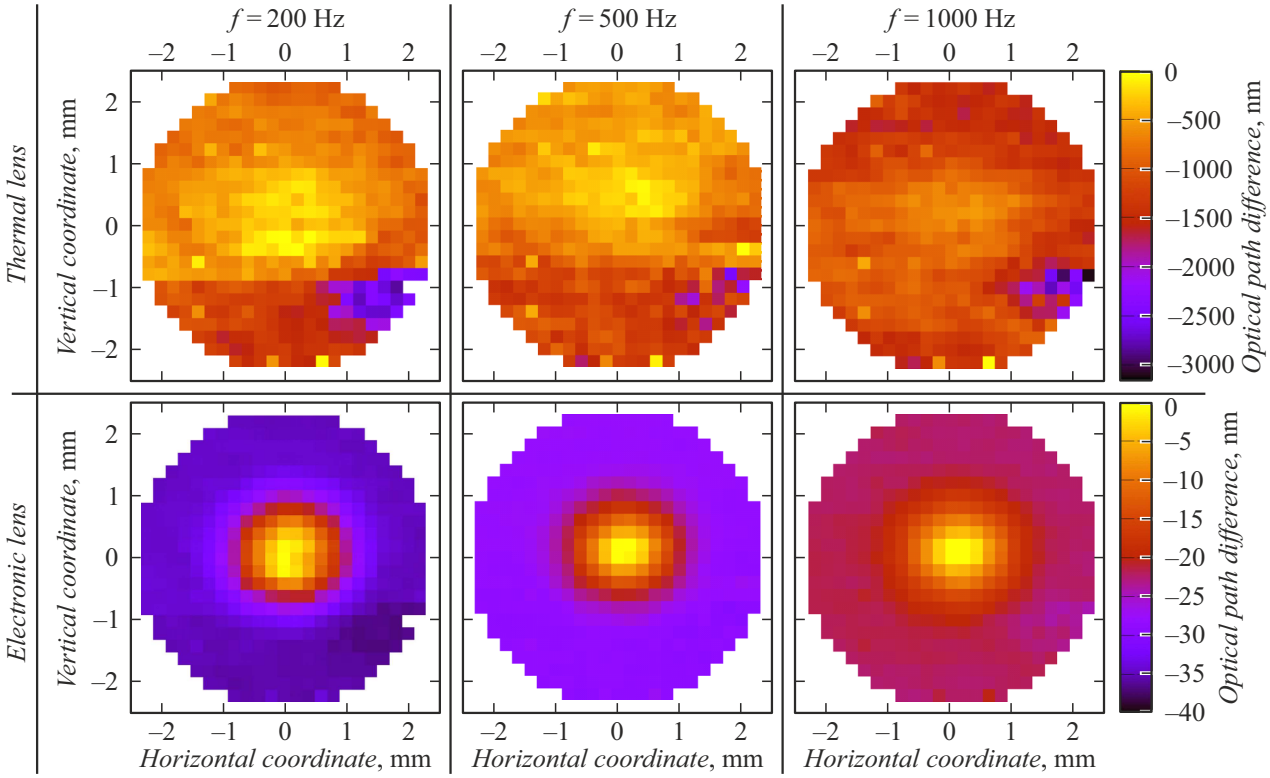

Optical path differences associated with the thermal component (top row) and electronic component (bottom row) for pulse repetition rates of 200, 500 and 1000 Hz.

The electronic component is associated with the working level lifetime. For laser active ions Yb^{3+} in crystalline matrices, the working level lifetime is about 1 ms. The technique proposed in [9] implies that the pump radiation is interrupted for a short time; thereat, the amplitude of the OPD electronic component decays orders of magnitude faster than that of the thermal one. Hence, though the OPD electronic and thermal components are determined from a single measurement, they are time resolved, which allows separation of their contributions. Thus, the technique enables studying the dynamics of radiation phase variations occurring under the influence of temperature and laser processes in the active element pumped region, including the case of radiation with a high pulse repetition rate.

The technique was applied in experimental investigation of wavefront distortions of radiation amplified in the active elements of a cryogenically cooled multi-disk multipass amplifier with an average diode pump radiation power of up to 200 W per element and pulse repetition rate of up to 1000 Hz. The amplifier active elements are diffusion welded YAG — Yb:YAG crystals (with the Yb^{3+} ion concentration of 10 at.%). The crystals are active mirrors in the form of disks with the 25 mm diameter, 3.75 mm doped region thickness, and 2 mm undoped region thickness [10].

The optical path differences presented in the figure were obtained from experimentally measured distributions of absorption and gain coefficients in the case of pumping by pulses with the peak power of 200 W, central wavelength of 936 nm, and pump spot profile diameter of ~ 2 mm. Radiation of the monochromatic scanning laser with the central wavelength of 1030 nm was focused into a spot $\sim 250\,\mu$m in diameter. The duty cycle did not change with changing pulse repetition rate and remained 3.6 in all the experiments.

When the pulse repetition rate varies while the duty cycle remains fixed, the active element temperature distribution changes only slightly. In this connection, the thermal OPD component also does not change qualitatively. At all the frequencies, OPD amplitude is ~ 2500 nm with the standard deviation of ~ 500 nm. The measured OPD has no clearly defined radial gradient, which makes impossible estimation of the thermal lens focal length. In all the experiments, the distributions exhibited a certain characteristic feature in their lower right quarters. We suggest that the presence of that feature is caused by either a defect in the active element or by features of attachment to the cryogenic cooler.

The OPD electronic component has a Gaussian profile. As the pump pulse repetition rate decreases, a characteristic increase in the OPD amplitude is observed due to an increase in the energy stored in the active element. In the case of pumping with a pulse repetition rate of 200 Hz, the maximum difference between the active element center and edge reaches ~ 40 nm, while in the case of pumping with the pulse repetition rate of 1000 Hz this difference does not exceed 30 nm. The estimate of the lens focal length is about 10 m.

Thus, the study has shown that, by using the laser scanning technique, it is possible to determine contributions of the electronic and thermal components to the refractive index variations, including those whose amplitudes differ by orders of magnitude. We have performed an analysis of the ratio between the thermal and electronic contributions to variations in the amplified radiation phase profile at the repetition rates of 200−1000 Hz and constant average power of the pump radiation. The amplitude of the thermal component of the wavefront distortions was shown to be two orders of magnitude higher than that of the electronic component.

Funding

The study was supported by the Russian Scientific Foundation (project № 23-22-00238).

Conflict of interests

The authors declare that they have no conflict of interests.

References

[1] V.Yu. Zheleznov, T.V. Malinskiy, S.I. Mikolutskiy, V.E. Rogalin, S.A. Filin, Yu.V. Khomich, V.A. Yamshchikov, I.A. Kaplunov, A.I. Ivanova, Tech. Phys. Lett., **47** (10), 734 (2021). DOI: 10.1134/S1063785021070282.
[2] V.E. Guseva, A.N. Nechay, A.A. Perekalov, N.N. Salashchenko, N.I. Chkhalo, Tech. Phys., **67** (8), 1002 (2022). DOI: 10.21883/TP.2022.08.54563.72-22.
[3] N.M. Al-Hosiny, A.A. El-Maaref, R.M. El-Agmy, Tech. Phys., **66** (12), 1341 (2021). DOI: 10.1134/S1063784221080028
[4] V.A. Petrov, G.V. Kuptsov, A.O. Kuptsova, V.V. Atuchin, E.V. Stroganova, V.V. Petrov, Photonics, **10** (7), 849 (2023). DOI: 10.3390/photonics10070849
[5] L.E. Zapata, M. Pergament, M. Schust, S. Reuter, J. Thesinga, C. Zapata, M. Kellert, U. Demirbas, A.-L. Calendron, Y. Liu, F.X. Kärtner, Opt. Lett., **47** (24), 6385 (2022). DOI: 10.1364/OL.476964
[6] E. Anashkina, O. Antipov, J. Opt. Soc. Am. B, **27** (3), 363 (2010). DOI: 10.1364/JOSAB.27.000363
[7] S. Chénais, F. Druon, S. Forget, F. Balembois, P. Georges, Prog. Quantum Electron., **30** (4), 89 (2006). DOI: 10.1016/j.pquantelec.2006.12.001
[8] I. Tamer, S. Keppler, M. Hornung, J. Körner, J. Hein, M.C. Kaluza, Laser Photon. Rev., **12** (2), 1700211 (2018). DOI: 10.1002/lpor.201700211
[9] G.V. Kuptsov, A.O. Konovalova, V.A. Petrov, A.V. Laptev, V.V. Atuchin, V.V. Petrov, Photonics, **9** (11), 805 (2022). DOI: 10.3390/photonics9110805
[10] G.V. Kuptsov, V.A. Petrov, V.V. Petrov, A.V. Laptev, A.O. Konovalova, A.V. Kirpichnikov, E.V. Pestryakov, Quantum Electron., **51** (8), 679 (2021). DOI: 10.1070/QEL17596.

Translated by EgoTranslating